

# Journal of Materials Chemistry A

Accepted Manuscript



This is an *Accepted Manuscript*, which has been through the Royal Society of Chemistry peer review process and has been accepted for publication.

*Accepted Manuscripts* are published online shortly after acceptance, before technical editing, formatting and proof reading. Using this free service, authors can make their results available to the community, in citable form, before we publish the edited article. We will replace this *Accepted Manuscript* with the edited and formatted *Advance Article* as soon as it is available.

You can find more information about *Accepted Manuscripts* in the [Information for Authors](#).

Please note that technical editing may introduce minor changes to the text and/or graphics, which may alter content. The journal's standard [Terms & Conditions](#) and the [Ethical guidelines](#) still apply. In no event shall the Royal Society of Chemistry be held responsible for any errors or omissions in this *Accepted Manuscript* or any consequences arising from the use of any information it contains.

Cite this: DOI: 10.1039/c0xx00000x

www.rsc.org/xxxxxx

ARTICLE TYPE

# Enhanced Photocatalytic Activity of Hydroxylated and N-doped Anatase Derived from Amorphous Hydrate

Chenyaoy Fan, Chao Chen, Jia Wang, Xinxin Fu, Zhimin Ren, Guodong Qian, Zhiyu Wang\*

Received (in XXX, XXX) Xth XXXXXXXXX 20XX, Accepted Xth XXXXXXXXX 20XX

DOI: 10.1039/b000000x

The hydrogenation on unmodified TiO<sub>2</sub> to create disorder layers on the surface of anatase nanocrystals (NCs) in order to enhance the photocatalytic activity of TiO<sub>2</sub> has been widely investigated in recent years. In this contribution, we prepared hydroxylated and N-doped anatase by controlling the degree of disorder of TiO<sub>2</sub> derived from amorphous hydrate through a traditional pathway of heating treatment, which induced various colours in appearance and outstanding photocatalytic activities. The traditional method by heating to prepare hydroxylated TiO<sub>2</sub> in this work is a reversed route comparing to the pathway by hydrogenation, which opens mind for the modification of nano-dimension semiconductors derived from amorphous hydrates.

## Introduction

As a versatile functional material, titanium dioxide (TiO<sub>2</sub>) has grabbed appreciable attention over the past decades, due to its powerful potential applications in photovoltaics, biomedicine, and photocatalysis,<sup>1-3</sup> which has been widely used in solar-hydrogen production, photocatalytic decomposition of organic pollutants, solar cells, and so forth.<sup>4-8</sup> However, one major issue for bare TiO<sub>2</sub> is the wide band-gap (typically 3.0~3.4eV), it makes TiO<sub>2</sub> effective only under UV light,<sup>9</sup> which accounts for less than 5% of the total solar irradiation. Another limitation of photocatalytic efficiency of unmodified TiO<sub>2</sub> is the low efficiency of separation of photo-generated electrons and holes.<sup>5</sup> So the methods for enhancing the photocatalytic activity of TiO<sub>2</sub> are mainly based on decreasing the band-gap and inhibiting the recombination of photo-generated electrons and holes.

In order to increase the limited optical absorption of TiO<sub>2</sub> under sunlight, narrowing the band-gap by introducing suitable heteroatoms has been actively pursued, there have been persistent efforts to vary the chemical composition of TiO<sub>2</sub> by adding controlled metal<sup>10-13</sup> or nonmetal (such as N<sup>14-16</sup>, C<sup>17, 18</sup>, F<sup>19</sup>, S<sup>20</sup>) impurities that generate donor or acceptor states in the band-gap. Liu at el. used a pre-doped interstitial boron gradient to weaken nearby Ti-O bonds for the easy substitution of oxygen by nitrogen, which prepared a red anatase TiO<sub>2</sub> microsphere with a band-gap gradient varying from 1.94eV on its surface to 3.22eV in its core by a conceptually different doping approach for harvesting the full spectrum of visible-light.<sup>21</sup> There also have numerous surface modifications been devoted to reduce the recombination of photo-generated electrons and holes, for example, TiO<sub>2</sub>/semiconductor composites,<sup>22, 23</sup> metallic doping,<sup>24</sup> heavy metal deposition upon TiO<sub>2</sub>.<sup>25</sup>

On the other hand, Tong at el. presented a doping-free strategy that assembled TiO<sub>2</sub> NCs together by interfacial Ti-Ti electronic bonding. The assembled TiO<sub>2</sub> NCs were bright yellow with narrowed band-gap and greatly enhanced visible light absorption.<sup>26</sup> Chen at el. first developed an alternative approach to improve visible and infrared optical absorption by engineering

the disorder on nanophase TiO<sub>2</sub> with hydrogenation treatment.<sup>27</sup> Hydrogenation on unmodified TiO<sub>2</sub> created a disordered layer on the nanoparticle (NP) surface. A shift in the onset of absorption that lower to about 1.0eV (~1200nm) in such disorder-engineered TiO<sub>2</sub> NPs was observed, accompanying with a dramatic colour change from white to black and substantial enhancement of solar-driven photocatalytic activity. After this report, the disordered black TiO<sub>2</sub> that created by hydrogenation treatment has triggered an explosion of interests in the application of TiO<sub>2</sub> in a diverse set of solar energy systems. Some studies proved that hydrogenation treatment induced the oxygen vacancies and Ti<sup>3+</sup> sites in TiO<sub>2</sub>, resulting in the band-gap narrowing and the separation of photo-generated electrons and holes, which remarkably improved the photocatalytic activity of TiO<sub>2</sub>.<sup>28-32</sup> While Chen at el. indicated that though Ti<sup>3+</sup> impurities and oxygen vacancy defects could turn white TiO<sub>2</sub> to yellow or blue,<sup>4, 33</sup> Ti<sup>3+</sup> here was not responsible for the visible and infrared absorption of black TiO<sub>2</sub>, and there was evidence of mid-gap states above the valence band maximum (VBM) due to the hydrogenation-engineered disorders.<sup>32</sup> In addition, Zheng at el. ascribed the enhanced photocatalytic activity to the improved optical absorption and efficient photo-generated electron-hole separation induced by the unique surface structure.<sup>34</sup> Naldoni et al. fabricated the black TiO<sub>2</sub> NPs with crystalline core/disordered shell morphology, and ascribed its narrowed band-gap to the synergistic presence of oxygen vacancies and surface disorder.<sup>35</sup> More examples showed the decisive role of defects such as oxygen vacancy in hydrogenated black TiO<sub>2</sub>. Wang at el.<sup>36</sup> and Zhang at el.<sup>37</sup> showed that oxygen vacancies served as electron donors and were primarily responsible for wide optical absorption and enhanced photocatalytic activity of TiO<sub>2</sub>. Liu at el. performed calculations based on the density functional theory (DFT) and the Perdew-Burke-Ernzerhof (PBE) functional, which indicated the lattice disorder in black TiO<sub>2</sub> could originate from the hydrogenation that helped to break up Ti-O bonds on the surface by forming Ti-H and O-H bonds, and the surface lattice disorder could blue-shift the VBM of TiO<sub>2</sub> by introducing mid-gap states while leaving its conduction band minimum (CBM) almost unchanged.<sup>38</sup>

However, there are some arguments about Chen et al.'s work. Leshuk et al. showed that hydrogenation-induced bulk defects could significantly degrade photocatalytic activity of black TiO<sub>2</sub>, which was significantly different from the original study by Chen et al., they proposed that high-temperature hydrogenation was the wrong approach to attempt to increase TiO<sub>2</sub> photocatalytic activity, as high temperatures were more likely to induce bulk vacancy defects.<sup>39</sup> Sun et al. also proved that heavy disorder was not observed under their hydrogenation conditions, probably due to the high temperature employed in the hydrogenation and showed the important role of predominant facets played in hydrogen incorporation.<sup>9</sup> The same point was mentioned by Yang et al.<sup>40</sup> and Gordon et al.<sup>41</sup> as well.

In the present work, we took amorphous hydrate that synthesized by Ti(SO<sub>4</sub>)<sub>2</sub> and ammonia water through one-step aqueous reactions as the precursor, followed by heating treatment to prepare hydroxylated anatase. The traditional pathway of wet chemistry with heating has been widely used in TiO<sub>2</sub> synthesis.<sup>42-44</sup> Here we used the simple traditional method instead of other modification processes such as hydrogenation for their multiple steps, harsh synthesis conditions, or expensive facilities.<sup>45</sup> Through which we prepared hydroxylated and N-doped anatase NCs with various colour and continuous changes in the structures and properties.

## Results and discussion

Powders of TiO<sub>2</sub> after heating treatment had significantly different colours in appearance. A photo of these kinds of colored TiO<sub>2</sub> that prepared after heating at a series of temperatures, as compared to original white TiO<sub>2</sub> without heating treatment, is shown in figure 1. Diffusive absorbance spectroscopy (figure 5a) reveals the much stronger optical absorption in visible-light and near infrared regions of brown TiO<sub>2</sub> that heated at 200°C comparing with TiO<sub>2</sub> heated at other temperatures, which indicates a large localized band bending for this sample. And for yellow TiO<sub>2</sub> that heated at 400°C, there is an abrupt change in optical absorbance at 455nm (2.73eV), which probably caused by a mid-gap state above the VBM. While gray TiO<sub>2</sub> heated at 600°C only has slightly enhanced visible-light absorption than original white TiO<sub>2</sub>, indicating a weak localized band bending. The treated TiO<sub>2</sub> with lower heating temperature had larger enhanced optical absorbance, which accorded with the darker colour in appearance.

The XRD patterns of the samples of colored TiO<sub>2</sub> (figure 2) demonstrate that their crystal phase had a continuous turning from amorphism to crystalline anatase with the increase of the heating temperature (200°C to 800°C). The percentages of crystallization calculated through the height of diffraction peak of each TiO<sub>2</sub> are displayed in the forth column of table 1. The XRD patterns proved that heating treatment could realize the structural control of TiO<sub>2</sub>, making the treated TiO<sub>2</sub> a mixed phase with different degrees of disorder. And if the heating temperature got further increasing, the crystal phase of TiO<sub>2</sub> would change to rutile at 1000°C (figure S1).

For the further research of the structural properties, we analyzed the chemical bonding of colored TiO<sub>2</sub> by X-ray photoelectron spectroscopy (XPS). The shapes of Ti 2p XPS spectra evidence no significant differences for original amorphous TiO<sub>2</sub> and treated TiO<sub>2</sub> after heating (figure 3a). The symmetric Ti 2p<sub>3/2</sub> peaks at 458.6eV and the Ti 2p<sub>1/2</sub> peaks at 464.2eV are attributed to the Ti<sup>4+</sup> of Ti-O bonds,<sup>46</sup> which demonstrates that Ti atoms had a similar bonding environment



**Figure 1.** A photo comparing the appearances of original white TiO<sub>2</sub> and colored TiO<sub>2</sub> heated at a series of temperatures. The colours of TiO<sub>2</sub> were white (original), dark brown (200°C), light brown (300°C), yellow (400°C), light yellow (500°C), gray (600°C), yellowish gray (700°C) and yellowish white (800°C).

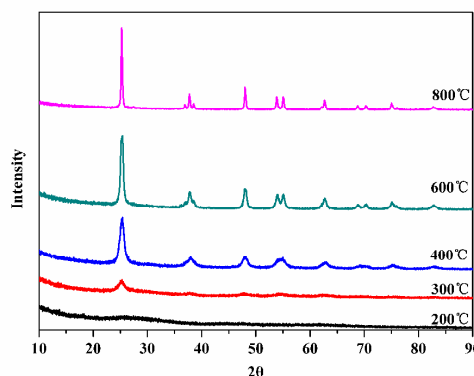


**Figure 2.** XRD patterns of colored TiO<sub>2</sub> heated at a series of temperatures.

**Table 1.** Structural parameters of original amorphous TiO<sub>2</sub> and hydroxylated anatase heated at a series of temperatures.

Sample	x <sub>1</sub> <sup>[a]</sup>	x <sub>2</sub> <sup>[b]</sup>	c% <sup>[c]</sup>	E <sub>g</sub> /eV
original	0.65	0.67	0	3.37
200°C	0.39	0.45	0	3.02
300°C	—	—	12	—
400°C	0.36	0.32	51	3.09
500°C	0.35	0.30	61	3.17
600°C	0.34	0.28	77	3.18
700°C	0.21	0.20	89	3.18
800°C	0.11	≈0	≈100	3.19

[a] The values of x (moisture content) in TiO<sub>2-x</sub>(OH)<sub>2x</sub> that drawn from XPS spectra.

[b] The values of x (moisture content) in TiO<sub>2-x</sub>(OH)<sub>2x</sub> that drawn from TG measurement.

[c] The percentages of crystallization of each sample.

before and after heating treatment. And there was no sign of Ti<sup>3+</sup>, which may take responsibility for the colored appearance and less crystallization of TiO<sub>2</sub>, abound.

However, the O 1s XPS spectra of each treated TiO<sub>2</sub> are quite different (figure 3b-3h). The single O 1s peak in each spectrum can be divided into two symmetric peaks: one locates at 530eV is

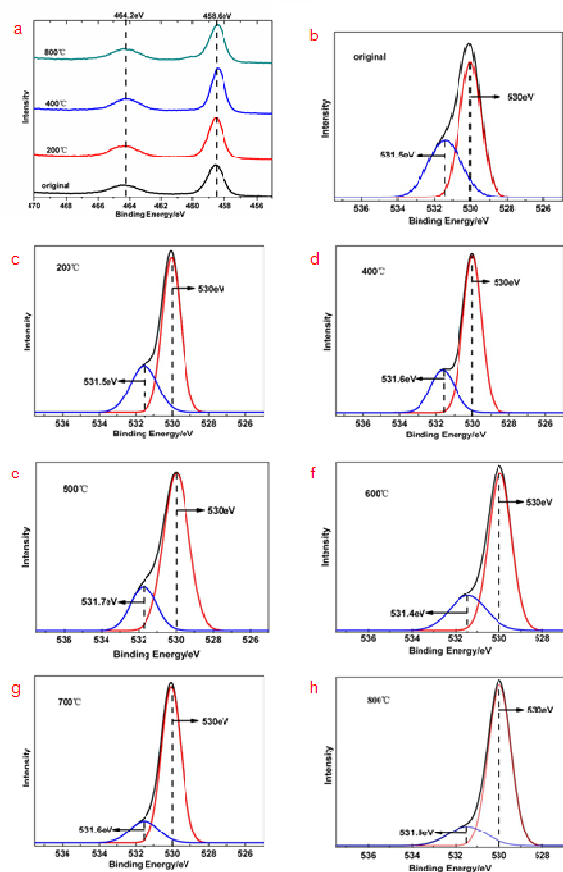


**Figure 3.** (a) Ti 2p XPS spectra of original amorphous TiO<sub>2</sub> and treated TiO<sub>2</sub> that heated at 200°C, 400°C and 800°C. (b)-(h) O 1s XPS spectra of original amorphous TiO<sub>2</sub> and hydroxylated TiO<sub>2</sub> that heated at a series of temperatures.

typical for the oxygen of Ti-O bonds in TiO<sub>2</sub>, the other one that locates between 530.9 eV and 532 eV is assigned to the oxygen of surface Ti-OH bonds.<sup>47</sup> As the area of Gauss peaks in each O 1s XPS spectrum represents the amount of Ti-O or Ti-OH bonds in treated TiO<sub>2</sub> respectively, it can be calculated that the ratio of Ti-O/Ti-OH bonds grew larger when TiO<sub>2</sub> heated at a higher temperature. The turning from Ti-OH bonds to Ti-O bonds in treated TiO<sub>2</sub> actually proved our samples of treated TiO<sub>2</sub> as hydroxylated anatase and indicated a process of dehydration in the hydroxylated anatase by heating. Based on the results of O 1s XPS, we should assume the accurate molecular formula of our samples of hydroxylated anatase as TiO<sub>2-x</sub>(OH)<sub>2x</sub>, in which the “x” represented the moisture content of each hydroxylated anatase. Combined with the relationships that a TiO<sub>2</sub> molecule contains two Ti-O bonds averagely and a H<sub>2</sub>O molecule was transformed by two Ti-OH bonds, it can be easily calculated that the value of x equals to the ratio of Ti-OH/Ti-O bonds. The calculated values of x of each hydroxylated anatase drawn from XPS spectra are displayed in the second column of table 1.

The Thermogravimetry (TG) was taken to confirm the viewpoint of dehydration in the structural change of hydroxylated anatase by heating. Based on the results in XRD patterns, the sample would be highly crystalline anatase when heated at 800°C. If we heated each sample at 800°C till constant weight, almost all the Ti-OH bonds could seem to be transformed to Ti-O bonds by dehydration and the losing weight was just the moisture content of each sample. The results of moisture content (values of x) are

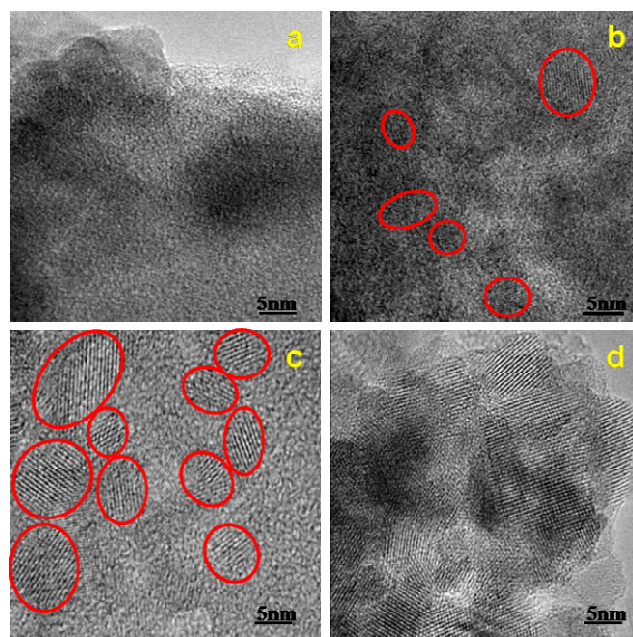


**Figure 4.** HRTEM images of treated TiO<sub>2</sub> that heated at 200°C (a), 300°C (b), 400°C (c), 800°C (d). The red circles mark the anatase NCs among the disordered structure.

displayed in the third column of table 1, which match well with the calculated values of x drawn from XPS spectra.

High Resolution Transmission Electron Microscopy (HRTEM) images in figure 4 show the process of the degree of disorder decreasing of hydroxylated anatase by heating. The amorphous brown TiO<sub>2</sub> heated at 200°C had totally disordered structure (figure 4a), and when heated at 300°C, there were crystal lattices emerging among the disordered structure (marked by red circles in figure 4b). The degree of crystallization of hydroxylated anatase was improved with the heating temperature increasing, making the grains grow up and the configuration of crystal lattices more regular (figure 4c and 4d). The images of HRTEM confirm the results of percentages of crystallization (the fourth column of table 1) that drawn from XRD spectra approximately and indicate the relationship between hydroxyl content and degree of disorder. These images also indicate that our synthesis of hydroxylated anatase derived from amorphous hydrate was just contrary to the pathway of Chen et al.’s work that engineered hydroxyls on the surface of anatase NCs, which prepared samples of hydroxylated anatase with a larger scale of disorder.

The density of states (DOS) of valance band of hydroxylated anatase was measured by VB XPS (figure 5b). And the direct optical transition of each sample was calculated using the equation:  $ah\nu = A(h\nu - E_g)^p$ , where  $a$  is the absorption coefficient,  $h\nu$  is the photon energy,  $E_g$  is the optical band-gap,  $p$  is assumed to be 0.5 for the direct transition and  $A$  is a constant concerning the transition probability. The direct transition of TiO<sub>2</sub> was calculated based on report<sup>48</sup>, and this transition was used to determine the  $E_g$  of our samples of hydroxylated anatase. The fifth column of table 1 displays the values of band-gap of hydroxylated anatase that transformed from the locations of optical absorption edges. Combined with the results of spectral absorbance and VB XPS spectra, we have constructed the schematic illustrations of DOS of hydroxylated anatase, which are shown in figure 5c. Because of the quantum size effect, the electronic energy levels of original amorphous TiO<sub>2</sub> were discrete instead of quasi-continuous energy bands,

Cite this: DOI: 10.1039/c0xx00000x

www.rsc.org/xxxxxx

ARTICLE TYPE

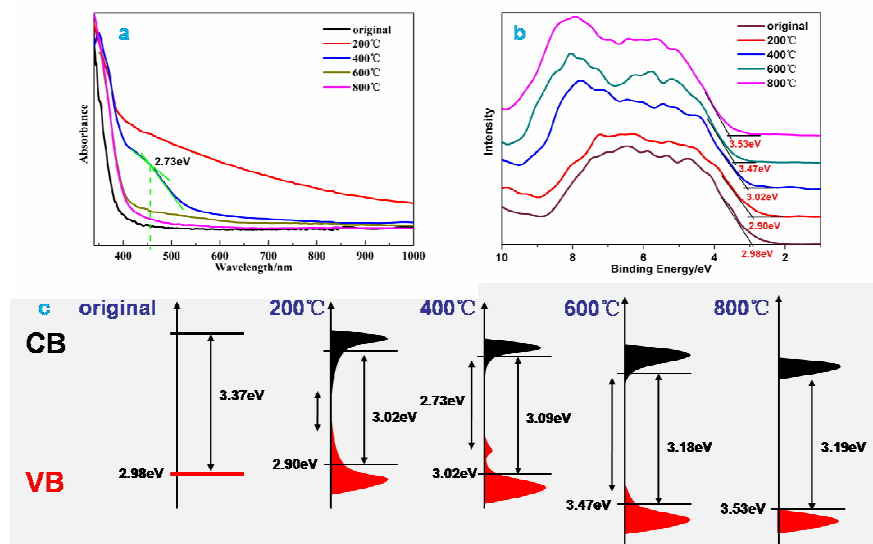


**Figure 5.** (a) Spectral absorbance of original amorphous TiO<sub>2</sub> and treated TiO<sub>2</sub> heated at a series of temperatures. The dash line indicates the abrupt change in absorbance of TiO<sub>2</sub> heated at 400°C. (b) VB XPS spectra of original amorphous TiO<sub>2</sub> and treated TiO<sub>2</sub> heated at a series of temperatures. The thin black lines indicate the locations of VBM of each TiO<sub>2</sub>. (c) Schematic illustrations of DOS of original amorphous TiO<sub>2</sub> and treated TiO<sub>2</sub> heated at a series of temperatures.

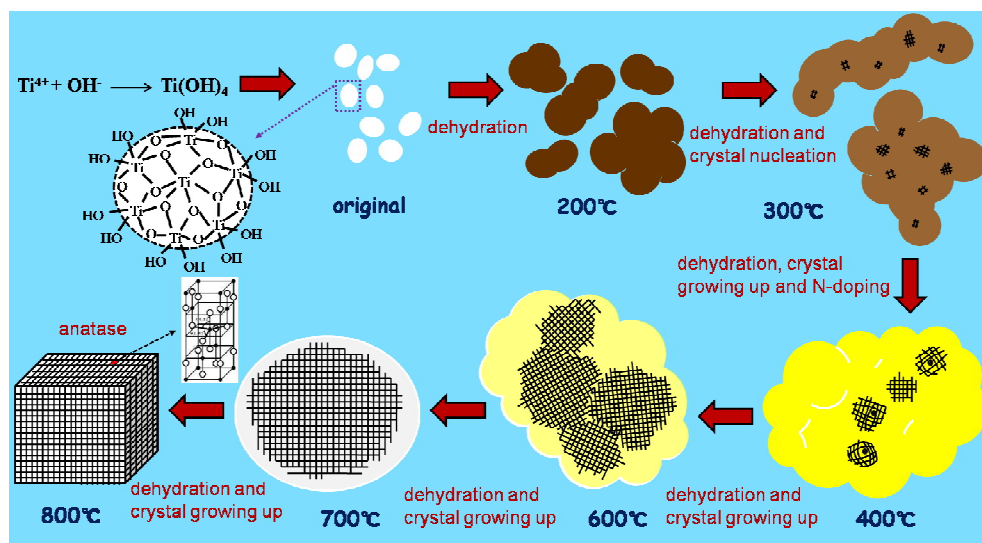


**Figure 6.** Schematic illustrations of frame work structure of original amorphous TiO<sub>2</sub> and hydroxylated anatase after heating treatment.

making the optical absorption edge of original amorphous TiO<sub>2</sub> have a blue-shift<sup>49, 50</sup> comparing with the other treated TiO<sub>2</sub> that had lower degree of disorder (figure 5a), and it showed a widest band-gap in all the samples. For amorphous TiO<sub>2</sub> that heated at 200°C, the optical absorption onset was over 1000nm, which suggested a conduction band tail arising from disorder<sup>27</sup> and a valance band tail blue-shifting further toward the vacuum level<sup>35</sup>, that would induce a much narrower band-gap. For hydroxylated anatase that heated at 400°C, the optical absorbance of its abrupt change at 455nm (2.73eV) was induced by the mid-gap states'

up-shifting the VBM. In order to understand the unique shape of UV-Vis spectroscopy of hydroxylated anatase heated at 400°C, we used KOH, NaHCO<sub>3</sub> and NH<sub>4</sub>HCO<sub>3</sub> respectively to replace ammonia water during synthesis (see the details in Supporting Information). The results of the contrast experiments (figure S2) indicated that the band tails were induced by the hydroxylation of TiO<sub>2</sub>, which made the brown colour. While the mid-gap state that caused the yellow colour of TiO<sub>2</sub> was attributed to nitrogen. The N 1s XPS spectra in figure 7a and the S 2p XPS spectra in figure 7b show that all samples of TiO<sub>2</sub> contained a certain amount of

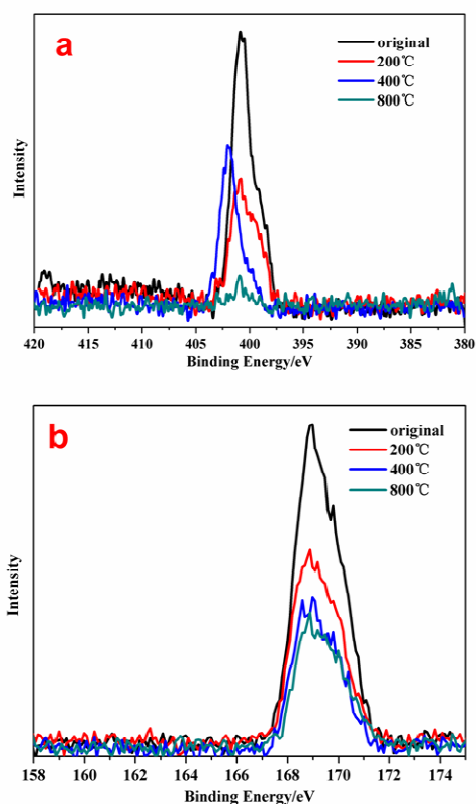


**Figure 7.** N 1s XPS spectra (a) and S 2p XPS spectra (b) of original amorphous TiO<sub>2</sub> and treated TiO<sub>2</sub> that heated at 200°C, 400°C and 800°C.

nitrogen and sulfate. The spectral peaks in both spectra only have decreases in intensity without any locational offset except the N 1s spectral peak of yellow TiO<sub>2</sub> that heated at 400°C, which could be divided into two peaks. The one that locates around 399–400eV is assigned to adsorbed radicals like NH<sub>3</sub> or NH<sub>2</sub>,<sup>14</sup> while the other one locates at 402eV is probably typical for interstitial N in TiO<sub>2</sub>, which indicates the nitrogen was doped into the crystal lattices of anatase under the condition of heating at 400°C and induced the mid-gap states above the VBM. And for hydroxylated anatase heated at 600°C, the doped N had been wiped off at high temperature, there were only slight band tails because of a little visible-light absorption and less degree of disorder, while no band tails existed for highly crystalline anatase heated at 800°C, and its band-gap (3.19eV) was typical for crystalline anatase.<sup>9, 37</sup> This continuous change of the energy band showed the effect of heating treatment on band-gap engineering by controlling the hydroxylation, N-doping and degree of disorder of hydroxylated anatase.

Considering the basic construction unit of TiO<sub>2</sub> was the TiO<sub>6</sub> octahedron, we could deduce the frame work structure of our hydroxylated anatase. Figure 6 shows the process of frame work structural changes from the original amorphous TiO<sub>2</sub> to crystalline anatase that heated at 800°C. It could be concluded from the results of XRD and XPS that the original amorphous TiO<sub>2</sub> consisted of the aggregates of several TiO<sub>6</sub> octahedrons by random dehydration synthesis of the hydroxyls on surfaces, which was the reason for its highest hydroxyl content and disordered structure. After heating at 200°C, the dispersed aggregates of TiO<sub>6</sub> octahedrons would constitute little chains or

circles by dehydration synthesis, and there would be crystal nucleus emerging among these connected aggregates when heated at 300°C. The frame work structure would expand from little chains or circles to disordered layers or bulks with the increasing heating temperature, accompanying with the anatase NCs' growing up among the connected aggregates. The doped-N (marked by black dots in figure 6) appeared at the interstitial sites of the crystal lattices when they were growing up at 400°C, making the lattices distortion, which would recover to be regular when heated at 600°C because of the removing of doped-N. Through the whole process of heating treatment, the aggregates of TiO<sub>6</sub> octahedrons would connect together by dehydration synthesis and expanded from lone islands to chains and bulks. Accompanied with the gather of aggregates, crystallization of anatase went on inside the disordered aggregates and would replace the disordered structure gradually to form an integrated three-dimensional network finally at 800°C. This process indicated that the heating treatment had an important control of the continuous changes in frame work structure of hydroxylated anatase.

The solar-driven photocatalytic activities of hydroxylated anatase were evaluated by monitoring the change in optical absorption of acid fuchsin (AF) solution during the process of its decomposing under illumination. The evaluation results are demonstrated in figure 8a and figure S3. For hydroxylated anatase that heated at 400°C~700°C, their solar-driven photocatalytic activities were enhanced successively by about 1.4, 1.75, 2.33 and 3.5 times than crystalline anatase that heated at 800°C respectively. The results apparently indicated that though amorphous TiO<sub>2</sub> itself did not show good solar-driven photocatalytic activities (figure S3), the disorder that induced by hydroxylation would enhance the solar-driven photocatalytic activity of anatase, and the degree of disorder in hydroxylated anatase that heated at 700°C made the best solar-driven photocatalytic activity.

If settled a colour filter on the light source, the visible-light-driven photocatalytic activities of the hydroxylated anatase could also be evaluated by monitoring the change in optical absorption of AF solution during the process of its decomposing under illumination. The evaluation results are shown in figure 8b and figure S3.

Compared to the results of solar-driven photocatalytic activity in figure 8a, the sequence of each sample's photocatalytic activity had big differences under visible-light-driven. The amorphous TiO<sub>2</sub> itself still had little visible-light-driven photocatalytic activity, and the degree of disorder in hydroxylated anatase that heated at 600°C made the highest visible-light-driven photocatalytic activity, followed by hydroxylated anatase that heated at 400°C and 500°C. While highly crystalline anatase (heated at 700°C and 800°C) had quite low visible-light-driven photocatalytic activities. This phenomenon was probably because that the reduction of organic molecules with the photocatalysis of TiO<sub>2</sub> under UV light was attributed to the formation of holes in valance band and hydroxyl radicals, and the disorder improved the efficiency of recombination of photo-generated electrons and holes. While there was no photo-generated hole under visible-light, TiO<sub>2</sub> was used to help to transmit the charges, and the mixed phase of amorphism and anatase was in favor of the separation of charges.<sup>51</sup> The disorder in hydroxylated anatase played a greater role under visible-light-driven photocatalysis than it did under solar-driven. Both of the results also suggested the N-doped anatase, which was once recognized as an efficient visible-light photocatalyst,<sup>14</sup> hardly had effective enhancement on photocatalytic activity due to the lower oxidation power of the photo-generated holes in nitrogen levels than those in the VB,<sup>52</sup>

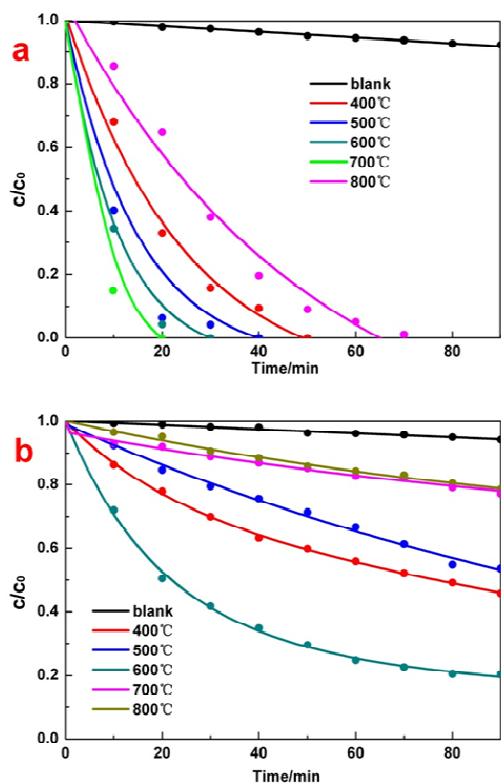


**Figure 8.** Evaluations of solar-driven (a) and visible-light-driven (b) photocatalytic activities (AF decomposition) of hydroxylated anatase heated at a series of temperatures.

and the mid-gap states induced by N-doping served as the recombination centers for the photo-generated charge carriers.<sup>53</sup>

Although original amorphous TiO<sub>2</sub> and amorphous TiO<sub>2</sub> that heated at 200°C had a quite different energy band structure, both of them did not present good photocatalytic activity neither under solar-driven nor visible-light-driven because the low degree of crystallization. However, based on the data of the surface area of some samples by BET measurement in table S1, TiO<sub>2</sub> with higher degree of disorder also had larger surface area, especially for original amorphous TiO<sub>2</sub> and amorphous TiO<sub>2</sub> that heated at 200°C. So despite their low activity of photocatalysis, the surface adsorption caused by the large surface area indicated these two kinds of TiO<sub>2</sub> can be used as effective adsorbent.

## Conclusions

In summary, we have shown a traditional method that using heating treatment to continuously change the degree of disorder by hydroxylation to prepare hydroxylated and N-doped anatase derived from amorphous hydrate that synthesized through one-step aqueous reaction, which is just a simple and reversed synthetic route comparing to the pathway by hydrogenation. Turning from Ti-OH bonds to Ti-O bonds by heating made the frame work structure of TiO<sub>2</sub> transform from disordered aggregates of TiO<sub>6</sub> octahedron to regular and integrated three-dimensional network, and their crystal phase from amorphism to crystalline anatase respectively. Hydroxylated anatase with higher degree of disorder had stronger optical absorption and narrower band-gap, which caused the darker colour in appearance. The nitrogen that adsorbed on the surface of

amorphous TiO<sub>2</sub> would be gradually wiped off by heating. But some of them were doped into the crystal lattices of hydroxylated anatase that heated at 400°C, making the yellow appearance. The doped-N vanished when heated at 600°C. Although amorphous TiO<sub>2</sub> only had low photocatalytic activity, the disorder induced by hydroxylation could enhance both solar-driven and visible-light-driven photocatalytic activities of hydroxylated anatase effectively, especially for visible-light-driven photocatalysis, while N-doped anatase showed no effective enhancement on photocatalytic activity. Besides, high degree of disorder gave the amorphous TiO<sub>2</sub> large surface area. This work provides a simple heating treatment method to continuously change the structure and properties of TiO<sub>2</sub> derived from amorphous hydrate, which can be applied to some other semiconductors to create hydroxylated NCs with various degrees of disorder. Through this method can we prepare materials with outstanding photocatalysis.

## Acknowledgements

The authors gratefully acknowledge the financial support for this work from the National Natural Science Foundation of China (Nos. 51229201, 51272231).

## Notes

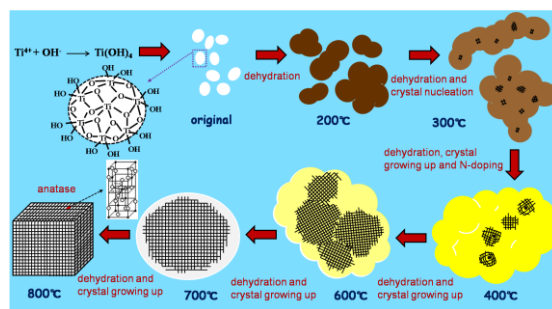
State Key laboratory of Silicon Materials, Department of Materials Science and Engineering, Zhejiang University, Hangzhou 310027, China. Tel: +86-13606637200; E-mail: wangzhiyu@zju.edu.cn

†Electronic Supplementary Information (ESI) available: [Detailed synthesis, experimental methods and additional material properties: XRD patterns of original amorphous TiO<sub>2</sub> and rutile that heated at 1000°C, photograph of contrasted samples, results of photocatalytic activity evaluations for original white TiO<sub>2</sub> and brown TiO<sub>2</sub> that heated at 200°C, table of values of surface area.] See DOI: 10.1039/b000000x/

## References

- Fujishima, A, Honda, K, *Nature* **1972**, 238, 37–38.
- Zhang, J, Xi, J, Ji, Z, *J. Mater. Chem.* **2012**, 22, 17700–17708.
- Jiang, X, Shi, A, Wang, Y, Li, Y, Pan, C, *Nanoscale* **2011**, 3, 3573–3577.
- Diebold, U, *Surf. Sci. Rep.* **2003**, 48, 53–229.
- Chen, X, Mao, S. S, *Chem. Rev.* **2007**, 107, 2891–2959.
- Fujishima, A, Zhang, X, Tryk, D. A, *Surf. Sci. Rep.* **2008**, 63, 515–582.
- Chen, X, Shen, S, Guo, L, Mao, S. S, *Chem. Rev.* **2010**, 110, 6503–6570.
- Sun, C. H, Liu, L. M, Selloni, A, Lu, G. Q, Smith, S. C, *J. Mater. Chem.* **2010**, 20, 10319–10334.
- Sun, C, Jia, Y, Yang, X, Yang, H, Yao, X, Lu, G. Q, Selloni, A, Smith, S. C, *J. Phys. Chem. C* **2011**, 115, 25590–25594.
- Hoffmann, M. R, Martin, S. T, Choi, W, Bahnemann, D. W, *Chem. Rev.* **1995**, 95, 69.
- Choi, W, Termin, A, Hoffmann, M. R, *Angew. Chem.* **1994**, 106, 1148.
- Yamashita, H, Harada, M, Misaka, J, Takeuchi, M, Ikeue, K, Anpo, M, *J. Photochem. Photobiol. A* **2002**, 148, 257–261.
- Kudo, A, Niishiro, R, Iwase, A, Kato, H, *Chem. Phys.* **2007**, 339, 104–110.
- Asahi, R, Morikawa, T, Ohwaki, T, Aoki, K, Taga, Y, *Science* **2001**, 293, 269–271.
- Miyauchi, M, Takashio, M, Tobimatsu, H, *Langmuir* **2004**, 20, 232–236.
- Mrowetz, M, Balcerski, W, Colussi, A. J, Hoffmann, M. R, *J. Phys. Chem. B* **2004**, 108, 17269–17273.
- Irie, H, Watanabe, Y, Hashimoto, K, *Chem. Lett.* **2003**, 32, 772–773.
- Sakthivel, S, Kisch, H, *Angew. Chem. Int. Ed.* **2003**, 42,

- 4908–4911.
19. Yu. J. C, Yu. J, Ho. W, Jiang. Z, Zhang. L, *Chem. Mater.* **2002**, 14, 3808–3816.
20. Ohno. T, Akiyoshi. M, Umebayashi. T, Asai. K, Mitsui. T, Matsumura. M, *Appl. Catal. A* **2004**, 265, 115–121.
21. Liu. G, Yin. L, Wang. J, Niu. P, Zhen. C, Xie. Y, Cheng. H, *Energy Environ. Sci.* **2012**, 5, 9603–9610.
22. Jiang. X, Wang. Y, Pan. C, *J. Alloys Compd.* **2011**, 509, L137–L141.
23. Zhang. Y, Fei. L, Jiang. X, Pan. C, Wang. Y, *J. Am. Ceram. Soc.* **2011**, 94, 4157–4161.
24. Zhao. W, Chen. C, Li. X, Zhao. J, *J. Phys. Chem. B* **2002**, 106, 5022–5028.
25. Wang. C, Pagel. R, Bahnemann. D. W, Dohrmann. J. K, *J. Phys. Chem. B* **2004**, 108, 14082–14092.
26. Tong. H, Umezawa. N, Ye. J, *Chem. Commun.* **2011**, 47, 4219–4221.
27. Chen. X, Liu. L, Yu. P. Y, Mao. S. S, *Science* **2011**, 331, 746–749.
28. Jiang. X, Zhang. Y, Jiang. J, Rong. Y, Wang. Y, Wu. Y, Pan. C, *J. Phys. Chem. C* **2012**, 116, 22619–22624.
29. Wang. W, Ni. Y, Lu. C, Xu. Z, *RSC Adv.* **2012**, 2, 8286–8288.
30. Zuo. F, Bozhilov. K, Dillon. R. J, Wang. L, Smith. P, Zhao. X, Bardeen. C, Feng. P, *Angew. Chem. Int. Ed.* **2012**, 51, 6223–6226.
31. Wang. W, Lu. C, Ni. Y, Song. J, Su. M, Xu. Z, *Catal. Commun.* **2012**, 22, 19–23.
32. Zuo. F, Wang. L, Wu. T, Zhang. Z, Borchardt. D, Feng. P, *J. Am. Chem. Soc.* **2010**, 132, 11856–11857.
33. Chen. X at el. *Sci. Rep.* **2013**, 3, 1–6.
34. Zheng. Z, Huang. B, Lu. J, Wang. Z, Qin. X, Zhang. X, Dai. Y, Whangbo. M, *Chem. Commun.* **2012**, 48, 5733–5735.
35. Naldoni. A, Allieta. M, Santangelo. S, Marelli. M, Fabbri. F, Cappelli. S, Bianchi. C. L, Psaro. R, Dal Santo. V, *J. Am. Chem. Soc.* **2012**, 134, 7600–7603.
36. Wang. G, Wang. H, Ling. Y, Tang. Y, Yang. X, Fitzmorris. R. C, Wang. C, Zhang. J. Z, Li. Y, *Nano Lett.* **2011**, 11, 3026–3033.
37. Zhang. Z, Bai. M, Guo. D, Wu. H, Hou. S, Zhang. G, *Chem. Commun.* **2011**, 47, 8439–8441.
38. Liu. L, Yu. P. Y, Chen. X, Mao. S. S, Shen. D. Z, *Phys. Rev. Lett.* **2013**, 111, 065505 (1–5).
39. Leshuk. T, Parviz. R, Everett. P, Krishnakumar. H, Varin. R. A, Gu. F, *ACS Appl. Mater. Interfaces.* **2013**, 5, 1892–1895.
40. Yang. H. G, Sun. C. H, Qiao. S. Z, Zou. J, Liu. G, Smith. S. C, Cheng. H. M, Lu. G. Q, *Nature* **2008**, 453, 638–641.
41. Gordon. T. R at el. *J. Am. Chem. Soc.* **2012**, 134, 6751–6761.
42. Yanagisawa. K, Ovenstone. J, *J. Phys. Chem. B* **1999**, 103, 7781–7787.
43. Yanagisawa. K, Ovenstone. J, *High Pressure Research* **2001**, 20, 79–85.
44. Shen. L, Bao. N, Zheng. Y, Gupta. A, An. T, Yanagisawa. K, *J. Phys. Chem. C* **2008**, 112, 8809–8818.
45. Wang. S, Zhao. L, Bai. L, Yan. J, Jiang. Q, Lian. J, *J. Mater. Chem. A.* **2014**, 2, 7439–7445.
46. Cappelletti. G, Ardizzone. S, Bianchi. C. L, Gialanella. S, Naldoni. A, Pirola. C, Ragaini. V, *Nanoscale Res. Lett.* **2009**, 4, 97–105.
47. McCafferty. E, Wightman. J. P, *Surf. Interface Anal.* **1998**, 26, 549.
48. Sheng. Y, Liang. L, Xu. Y, Wu. D, Sun. Y, *Opt. Mater.* **2008**, 30, 1310–1315.
49. Ohtani. B, Ogawa. Y, Nishimoto. S, *J. Phys. Chem. B* **1997**, 101, 3746–3752.
50. Liu. T. X, Li. F. B, Li. X. Z, *J. hazard. Mater.* **2008**, 152, 347–355.
51. Chen. C, Ma. W, Zhao. J, *Chem. Soc. Rev.* **2010**, 39, 4206–4219.
52. Irie. H, Watanabe. Y, Hashimoto. K, *J. Phys. Chem. B* **2003**, 107, 5483–5486.
53. Lin. M, Inde. R, Nishikawa. M, Qiu. X, Atarashi. D, Sakai. E, Nosaka. Y, Hashimoto. K, Miyauchi. M, *ACS NANO*, **2014**/DOI: 10.1021/nn502247x.



Controlling the degree of disorder to prepare hydroxylated and N-doped TiO<sub>2</sub> with various colours and enhanced photocatalytic activity.

Controlling the degree of disorder to prepare hydroxylated and N-doped TiO<sub>2</sub> with various colours and enhanced photocatalytic activity.